THE ASTROPHYSICAL JOURNAL, 219:105–113, 1978 January 1

CO OBSERVATIONS ALONG AN IONIZATION FRONT OF THE CALIFORNIA NEBULA (NGC 1499)

DEBRA MELOY ELMEGREEN AND BRUCE G. ELMEGREEN
Center for Astrophysics, Harvard College Observatory and Smithsonian Astrophysical Observatory
Received 1977 April 4; accepted 1977 June 20

ABSTRACT

A dark cloud on the northern edge of the California Nebula (NGC 1499) has been mapped at 3′ resolution in ^{12}CO and sampled in ^{13}CO and CS. The conversion of ^{13}CO to H_2 column densities is discussed. Some velocity structure exists in each of two isolated fragments that are outlined by the ^{12}CO temperature contours. Irregularities of the southern cloud boundary (at the ionization front) are attributed to an instability that may result from the time-dependent flux of the runaway star ξ Persei, which ionizes the H II region. An unresolved globule or filament close to the ionization front may have become separated from the main cloud as the result of a Kelvin-Helmholtz instability.

Subject headings: interstellar: molecules — nebulae: individual

I. INTRODUCTION

The California Nebula (NGC 1499) is an emission region at a distance of 350 pc (Bohnenstengel and Wendker 1976) which covers an area $\sim 1°$ by $4°$ along the northern boundary of the Perseus OB2 association. The primary source of ionization is the runaway star ξ Persei (Bohnenstengel and Wendker 1976; Shinohara and Ishida 1976). A large dark cloud, including Lynds 1449 (Lynds 1962), borders the nebula and extends as far as 2° to the north in some places. The $\sim 2°$ long interface between the H II region and the neutral cloud contains numerous bright rims (Pottasch 1956) which combine to form a long ionization front.

Because of the possibility that the ionization of NGC 1499 has occurred only recently, when ξ Per has been close enough to interact with the dark cloud, the early stages in the development of an ionization front may be evident. Instabilities that occur in time-dependent radiation fields also may be present (Kahn 1958). Here we summarize CO observations of the part of the molecular cloud adjacent to NGC 1499. Some implications for theoretical work on ionization fronts are discussed.

II. OBSERVATIONS

An area measuring 40′ by 70′ that lies along the interface between NGC 1499 and L1449 was mapped at 3′ or 1.′5 intervals with emission from the $J = 1 \rightarrow 0$ transition of ^{12}CO (2.6 mm). The observations were made in 1976 December and 1977 February with the 16 foot (5 m) telescope of the Millimeter Wave Observatory in Fort Davis, Texas.[1] The half-power beamwidth (HPBW) of the antenna is 2.′7 at this wavelength. Forty frequency channels were used, with a velocity resolution of 0.65 km s^{-1} for ^{12}CO. An integration time of 5 minutes (split equally between signal and comparison sidebands) for ^{12}CO and 15 minutes for ^{13}CO gave minimum detectable temperatures of about 2 and 1 K, respectively. Antenna temperatures were converted to brightness temperatures by using the calibration of Davis and Vanden Bout (1973).

Several areas were sampled near NGC 1499 in addition to that shown in Figure 1*a*. A small region around $\alpha(1950.0) = 3^h57^m$, $\delta(1950.0) = 37°00'$, consisting of about 20 points, showed peak emission of ~ 10 K at a velocity of ~ 3 km s^{-1}. We do not discuss this region further. Another region around $\alpha = 3^h59^m$, $\delta = 36°35'.5$ was observed in ^{12}CO, but there was no indication of any emission within a limit of 2 K. This is consistent with the extinction maps of Lynds (1969), where a dark cloud is shown only above the northwestern half of the nebula. Points at 3′ intervals were also mapped along a vertical strip from $\alpha = 3^h54^m45^s$, $\delta = 36°50'00''$, south to $\delta = 36°15'00''$. This strip includes some of the filamentary structure seen in the photograph of Figure 1*a*. The results showed no positive detection of ^{12}CO within a 3 K limit.

Our primary studies of CO were focused on the northwest boundary of the optical nebula, at the position of L1449. Here, corrected, equivalent Rayleigh-Jeans temperatures peak to 17 K in several isolated regions. The overall structure near the ionization front is shown in Figure 1*b*, where contours of ^{12}CO corrected temperatures are superposed on a

[1] The Millimeter Wave Observatory is operated by the Electrical Engineering Research Laboratory, University of Texas at Austin, with support from the National Aeronautics and Space Administration, the National Science Foundation, and McDonald Observatory. The instrumentation used for spectral-line observations with this antenna was developed jointly by the University of Texas, Bell Telephone Laboratories, and the Radio Astronomy Division of the Center for Astrophysics.

red plate from the Palomar Observatory Sky Survey (POSS). The CO is confined to two spatial components which are separated by a channel with no detectable ^{12}CO. The southern edge of the components follows the border of the optical nebula rather well. The radio continuum map of Bohnenstengel and Wendker (1976) shows that very little thermal emission comes from obscured regions. The bifurcation in the ^{12}CO contours does not show up on the POSS at all, although there is an indication from star counts that the extinction is slightly less where the CO intensity drops.

Several velocity components are present in the region studied. The dominant component has a centroid velocity of -4.8 ± 0.9 km s^{-1} east of the bifurcation, and -2.7 ± 0.9 km s^{-1} to the west. Velocity gradients are present in each fragment, however, with a tendency for the southern emission to be redshifted relative to the gas in the north. In the east, the velocity decreases from -4.4 ± 0.4 km s^{-1} at the southern edge of the cloud to -6.4 ± 0.4 km s^{-1} at the northern limits of the contours; in the west, the 15 K CO peak which juts into the H II region has a centroid velocity of -1.7 ± 0.2 km s^{-1}, compared with -3.1 ± 0.8 km s^{-1} in the north. In all cases, the systematic shift of centroid velocities is comparable to the full width at half-maximum (FWHM) of the lines, which averages 1.9 ± 0.5 km s^{-1} throughout both parts of the cloud.

An additional weak ($\sim$5 K) component was observed at $\sim +3$ km s^{-1} at two dozen isolated locations in the eastern and western cloud segments. About a third of these points occur in the area near $\alpha = 3^h53^m27^s.6$, $\delta = 37°11'56''.4$—i.e., along the eastern periphery of the hole seen in Figure 1*b*. In this same eastern fragment, north of $\delta = 37°20'$, the main line occurs between -4 km s^{-1} and -6 km s^{-1}, and becomes gradually weaker with increasing declination, until it eventually disappears at $\delta \approx 37°30'$. The $+3$ km s^{-1} line persists at about constant intensity (5–7 K) to the north until $\delta \gtrsim 37°35'$, where it also disappears. A point further to the north, at $\delta \approx 38°$, showed no CO emission in the range -14 km s^{-1} to $+10$ km s^{-1}. North of $\delta \approx 37°30'$, in the western cloud fragment, there is no $+3$ km s^{-1} feature at all; but the main line at -3 km s^{-1} persists at 5 K at least as far north as 37°35′.

We also searched for H_2O masers using the 36.5 m Haystack Observatory[2] 22 GHz system in 1977 February. Approximately 70 points near the edges of the bifurcated regions, as well as the ^{12}CO peak emission spots, were scanned with single beam spacings of 1′. No emission was detected to a limit of 0.3 K.

Fifteen select points in the region mapped were observed in ^{13}CO, in addition to some of the northern regions where the $+3$ km s^{-1} component appears. We then derived ^{13}CO column densities using the method of Knapp *et al.* (1977). The thermal temperature of ^{12}CO is assumed to equal the excitation temperature, T_{ex}, given by

$$T_{ex} = 5.54\left\{\ln\left[1 + \frac{5.54}{T_A(^{12}\mathrm{CO}) + 0.817}\right]\right\}^{-1} \quad (1)$$

for frequency $\nu = 115.27$ GHz and observed antenna temperature T_A. This is equivalent to assuming that ^{12}CO is optically thick and that the source size is larger than the antenna beamwidth. Since the temperature calibration is done with a rotating chopper wheel, the effective beam efficiency is unity.

If one assumes that ^{13}CO is thermalized at the same temperature as ^{12}CO, the optical depth of ^{13}CO is given by

$$\tau(^{13}\mathrm{CO}) = -\ln\left[1 - T_A(^{13}\mathrm{CO})/T_A(^{12}\mathrm{CO})\right] \quad (2)$$

for ^{13}CO frequency 110.20 GHz. The partition function for ^{13}CO is within 2% of the value $0.378(T_{ex} + 0.91)$ for T_{ex} between 10 and 20 K, so the column density becomes

$$N(^{13}\mathrm{CO}) = \frac{2.31 \times 10^{14}\tau(^{13}\mathrm{CO})\Delta v(^{13}\mathrm{CO})(T_{ex} + 0.91)}{1 - \exp(-5.29/T_{ex})}, \quad (3)$$

where Δv is the FWHM of the ^{13}CO line, in km s^{-1}.

The ^{13}CO column densities obtained from our observations are presented in Table 1. They range from values less than 1.1×10^{15} cm^{-2} to the maximum observed value of 6.5×10^{15} cm^{-2}.

III. ESTIMATES OF THE H_2 COLUMN DENSITIES

The conversion from ^{13}CO to H_2 column densities depends on the ^{12}C/^{13}C isotope ratio, the degree of fractionation of CO (Langer 1977), and the depletion of carbon relative to the cosmic abundance. Several empirical values of $\epsilon = N(^{13}\mathrm{CO})/N(H_2)$ have been determined from a comparison of CO data with star counts and extinction measurements (Encrenaz, Falgarone, and Lucas 1975; Dickman 1975; Tucker *et al.* 1976). The results cluster around the value

$$\epsilon \approx 2 \times 10^{-6}, \quad (4)$$

with a 50% scatter. Using radio recombination lines, Chaisson (1975) determines the C/H ratio in a carbon Strömgren sphere in the ρ Oph cloud. His value implies a factor of $\sim$6 for carbon depletion onto grains. If ^{12}CO/^{13}CO = 40, as in Wannier *et al.* (1976), then the density ratio $n(^{13}\mathrm{CO})/n(H_2) \approx 3 \times 10^{-6}$, which gives the same ϵ if most of the gaseous carbon in other clouds with similar depletion is in the form of CO.

Using the tables of van Rhijn (1929), we applied the star count method of Dickman (1975) to the western 10 K contour. The red POSS plate in Figure 1 shows roughly one-third as many stars in this 10 K contour as in an equal area near $\alpha = 3^h51^m$, $\delta = 37°00'$. The red extinction is then about 1.4 mag, and the visual

[2] The Haystack Observatory in Westford, Massachusetts, is operated by the Northeast Radio Observatory Corporation, with support from the National Science Foundation.

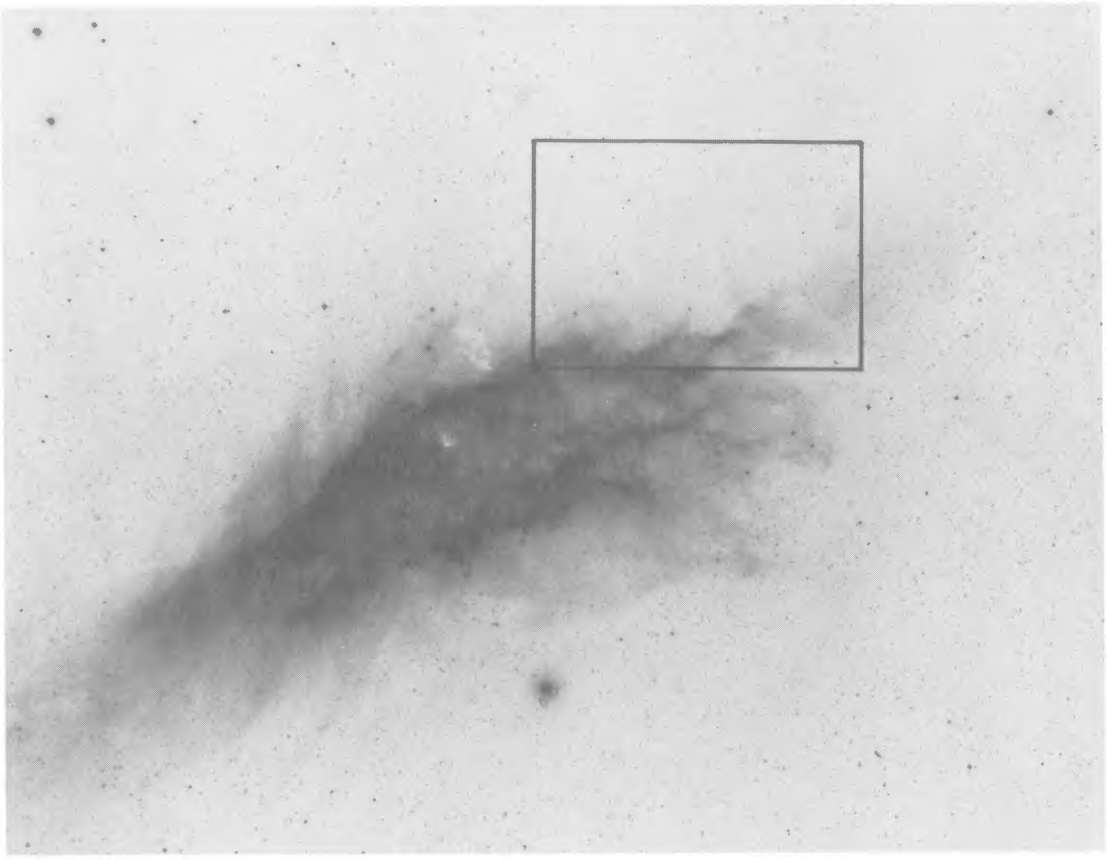

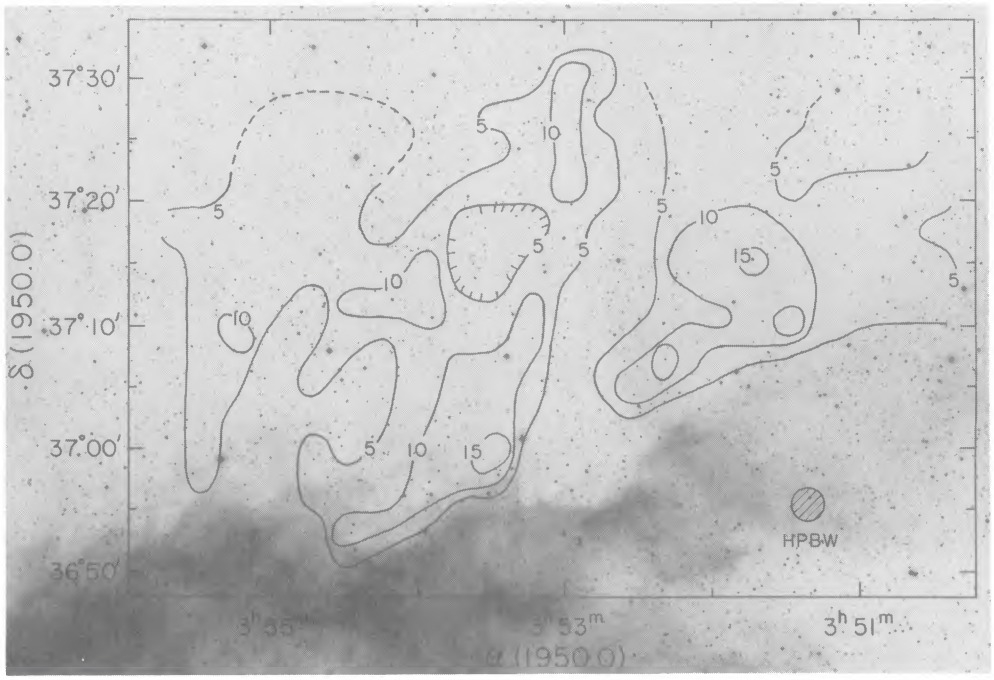

FIG. 1*a* (*top*).—The region mapped in carbon monoxide, indicated by a rectangle, is shown superposed on the red plate of NGC 1499 from the Palomar Observatory Sky Survey. The ionizing star, ξ Per, is south of the nebulosity.

FIG. 1*b* (*bottom*).—Contours of ^{12}CO corrected temperatures are superposed on an enlargement of the northwestern edge of NGC 1499. Contour divisions denote regions of T_A = 5, 10, and 15 K. Region A, mentioned in the text, is at $\alpha = 3^h53^m27^s.6$, $\delta = 36°59'56''.4$; Region B is at $\alpha = 3^h52^m20^s.0$, $\delta = 37°07'26''.4$.

TABLE 1

OBSERVATIONS OF ^{13}CO

COORDINATES		$T(^{12}CO)$*	$T(^{13}CO)$*	$\Delta v(^{13}CO)$†	$N(^{13}CO)$	$N(H_2)$
α(1950.0)	δ(1950.0)	(K)	(K)	(km s^{-1})	($\times 10^{15}$) (cm^{-2})	($\times 10^{20}$) (cm^{-2})
3^{h}51^{m}42^s.4	37°11′56″.4	10.7	2.4	1.8	5.1	26
3 51 42.4	37 14 56.4	16.0	2.9	1.5	5.9	30
3 51 57.4	37 07 56.4	7.6	1.3	1.9	2.6	13
3 51 57.4	37 08 56.4	10.8	1.4	1.7	2.7	13
3 52 20.0	37 04 26.4	9.3	1.5	1.4	2.3	11
3 52 20.0	37 05 56.4	15.1	2.2	1.3	3.7	19
3 52 20.0‡	37 07 26.4‡	17.0	1.6	1.8	3.9	19
3 52 20.0	37 08 56.4	9.0	< 1.0	...	< 1.6	< 7.8
3 52 57.6	37 20 56.4	12.8	1.0	1.2	1.4	7.0
3 53 27.6§	36 59 56.4§	15.5	3.4	1.4	6.5	32
3 53 42.6	37 05 56.4	10.5	1.4	1.2	1.9	9.2
3 53 57.7	37 05 56.4	9.0	< 0.7	...	< 1.1	< 5.4
3 53 57.7	37 11 56.4	13.1	1.4	2.3	3.8	19
3 54 12.7	36 55 26.4	6.1	1.2	1.5	1.8	9.2
3 54 57.8	37 14 56.4	8.7	< 1.0	...	< 1.5	< 7.8
3 54 57.8	37 23 56.4	6.0‖	1.5‖	1.7	2.7	13
3 55 28.0	37 26 56.4	3.5	1.0	1.3	1.4	7.0
		7.1‖	1.3‖	2.4	3.2	16

* Signal-to-noise ratio is ~6 for ^{12}CO and ~3 for ^{13}CO temperatures.

† Full width at half-maximum is accurate to ~1 channel, which corresponds to 0.68 km s^{-1} for ^{13}CO.

‡ Region B.

§ Region A.

‖ v(LSR) ≈ +3 km s^{-1} (see text for discussion).

extinction is about 1.7 mag. Using a conversion factor to H_2 of 1.25×10^{21} cm^{-2} mag^{-1} (Jenkins and Savage 1974), we calculate an average H_2 column density of around 2.1×10^{21} cm^{-2}. The ^{13}CO column densities at two points near the center of this region have an average of 5.5×10^{15} cm^{-2} from Table 1; so we obtain $\epsilon \approx 3 \times 10^{-6}$, in rough agreement with the other determinations.

There may be a problem with the application of equation (4) to regions with extremely low visual extinction (Encrenaz *et al.*; Knapp and Jura 1976; Langer 1977), although Dickman (1975) found evidence for this conversion factor at $A_V \approx 1$ mag. Equation (4) may also break down at high A_V, where slower chemical processes make ϵ time-dependent (Langer 1977; Oppenheimer and Dalgarno 1975) and where greater depletion of carbon onto grains may occur. Large UV shielding limits the formation of both C^+ (by photoionization) and positively charged grains (by photoejection), so carbon could more readily impact and adhere to grains where A_V is large. This would tend to lower ϵ for regions of high extinction, as would the time dependence of CO formation.

It has been suggested that CO column densities in Sgr B2 and in the M17 cloud complex, both of which contain more than $10^6 M_\odot$, may be interpreted by using lower values of ϵ. Scoville, Solomon, and Penzias (1975) point out that a value of ϵ as high as 6×10^{-6} would make the ^{13}CO lines in Sgr B2 unreasonably opaque, and they suggest a lower value of 1×10^{-6}. For M17, Elmegreen and Lada (1976) used absolute density measurements as a check on ϵ. A value of 7×10^{-7} was shown to give agreement between H_2 space densities estimated from the ^{13}CO column densities and space densities obtained from a more detailed radiative-transfer analysis of other molecular species, like HCN, H_2CO, and CS (Gottlieb *et al.* 1975; Lada 1976). Of course, the density-dependent molecular transitions may originate in a small core with unknown line-of-sight depth, in which case their low value of ϵ may reflect an improper conversion of ^{13}CO column densities to space densities.

For the cloud in Figure 1*b*, however, the extinction is probably low enough everywhere to allow us to use equation (4) with some confidence. The H_2 column densities corresponding to this ϵ and to the derived values of $N(^{13}CO)$ are given in Table 1. Several implications of this value of ϵ are now discussed.

We observed several points of Figure 1 in the $J = 3 \rightarrow 2$ transition of CS (147 GHz) to determine absolute space densities according to the method of Penzias *et al.* (1971). A detection was made at $\alpha = 3^h53^m27^s.6$, $\delta = 36°59'56''.4$ (hereafter Region A), with a corrected temperature of

$$T_A(\mathrm{CS}) = 1.2 \pm 0.4 \text{ K} .$$

If one assumes for the moment that this transition is thermalized in Region A and that the CS source fills the beam (HPBW = 2′.1), then the CS excitation temperature is 4.4 ± 0.5 K for a kinetic temperature of 19 K. Using Penzias *et al.* (1971), we then obtain $n(H_2) = 3.1 \pm 0.8 \times 10^5$ cm^{-3}. If $N(H_2) = 3.2 \times 10^{21}$ cm^{-2} (from Table 1) and the space density is as high as 3.1×10^5 cm^{-3}, then the line-of-sight depth of the molecular region must be only 1.0×10^{16} cm,

which corresponds to an angular size of 1.″9 at the distance of ξ Per, 350 pc (Bohnenstengel and Wendker 1976). This implies either that the CS source is highly flattened in the line of sight or that beam dilution is important. However, a CS source with total CS column density less than 2.5×10^{13} cm^{-2}, for the observed FWHM of 1.5 km s^{-1}, will have optical depth unity for the $J = 3 \rightarrow 2$ transition observed here (see Penzias *et al.* 1971). This would occur in a region where $N(H_2) \approx 2.0 \times 10^{21}$ cm^{-2}, if more than $\sim 5 \times 10^{-4}$ of the cosmic abundance of sulfur is in the form of CS. In that case, photon excitation will compete with collisional excitation and the density requirement for the observed CS intensity will be less (e.g., Liszt and Linke 1975).

Another way to estimate space densities is to consider the possible balance of pressure across the ionization front. This pressure balance would be achieved over a length $L = 0.27$ pc (1 CO beamwidth) in the time $L/c \approx 1 \times 10^6$ years for c equal to the isothermal sound speed; or $L/(\Delta v/2) \approx 3 \times 10^5$ years for a turbulent velocity equal to the observed line width; or a smaller time, L/v_A, for some Alfvén velocity $v_A > \Delta v$ (see, e.g., Arons and Max 1975). The pressure exerted on the neutral gas by the bright rim ranges between $2.1 n_e k T_e$ and twice this value, depending on the importance of kinematic pressure from the outflow of ionized gas (Spitzer 1968). The pressure in the neutral gas is ρc^2, $\rho(\Delta v/2)^2$, or $\rho {v_A}^2$ for thermal, turbulent, or magnetic pressure, respectively. If one uses the lower value of external pressure with a temperature $T_e = 8000$ K, electron density $n_e = 45$ cm^{-3} from Bohnenstengel and Wendker (1976), and a temperature in Region A of 19 K, then the external pressure will balance internal *thermal* pressure, if

$$n(H_2) \approx 4 \times 10^4 \text{ cm}^{-3} .$$

External pressure will balance internal *turbulent* pressure with $\Delta v/2 = 1.1$ km s^{-1}, if

$$n(H_2) \approx 2 \times 10^3 \text{ cm}^{-3} .$$

Balance of external and magnetic pressure with $v_A > \Delta v$ could give a lower internal density, if the magnetic field is in the plane of the ionization front. For any other orientation of the field, magnetic pressure will not be important at the front.

If the value of $n(H_2)$ from thermal pressure is used with $N(^{13}CO)$ at the peak of Region A, then either $\epsilon < 2 \times 10^{-7}$ or the line-of-sight depth of the region near the ionization front must be much less than a beamwidth; for $\epsilon \approx 2 \times 10^{-6}$, this depth is only 8×10^{16} cm. The second value of $n(H_2)$ (from turbulent pressure) corresponds to a 0.5 pc depth, or 1.8 times the beamwidth, if $\epsilon \approx 2 \times 10^{-6}$. A smaller value of $n(H_2)$, possible in the case of strong magnetic fields, allows the line-of-sight depth to be increased for a given value of ϵ. Thus Region A may or may not be resolved, depending on the internal density and, therefore, on the source of internal pressure.

Another region of interest is located at $\alpha = 3^h52^m20^s0$, $\delta = 37°07'26''.4$ (hereafter Region B). Here turbulent pressure will balance the same external pressure as in Region A, if the line-of-sight depth is only 0.2 pc, or 0.7 of a beamwidth (from Table 1). An even smaller dimension for Region B will be obtained, if internal thermal pressure balances the external pressure. We conclude from pressure arguments that Region B may be unresolved, unless the internal Alfvén velocity is significantly greater than the observed line width. We determined the column density of ^{13}CO at 1.′5 intervals on a N-S line across the temperature peak at Region B. The resultant profile of $N(^{13}CO)$ across this region provides an estimate of the region's N-S dimension. The full width at half-maximum of this profile is $\sim 4'.0$. Since ^{12}CO contours around Region B make an angle of $\sim 50°$ to the N-S line, the protrusion has an apparent width of 4 sin (50°) = 3.′1. Deconvolving this from a 2.′7 beam, we obtain an estimated source width of $\sim 1'.5$, which is about one-half of the beam. This corresponds to a dimension of 0.15 pc. Thus Region B is probably unresolved.

If this is the case, the excitation temperature of Region B will be larger than that derived from equation (1) by using the observed ^{12}CO temperature. If it is assumed that the intrinsic intensity (corrected for blackbody radiation) of the ^{12}CO source scales with $f^{-\alpha}$, the true excitation temperature is given by

$$T_{ex} = 5.54 \left\{ \ln \left[1 + \frac{5.54 f^{\alpha}}{T_A(^{12}CO) + 0.817 f^{\alpha}} \right] \right\}^{-1} \quad (5)$$

for $f(<1)$ equal to the fraction of the beam which the source subtends, and $\alpha = 2$ for a spherical unresolved source or $\alpha = 1$ for a filamentary (linear) source. Taking $T_A(^{12}CO) = 17$ K and $f = \frac{1}{2}$ for Region B, we obtain $T_{ex} = 72$ or 38 K, respectively. Since both the ^{12}CO and the ^{13}CO intensities (corrected for blackbody radiation) scale the same way with source size, the optical depth of ^{13}CO is independent of f. The column density of ^{13}CO in an unresolved source now follows from equation (3), with T_{ex} from equation (5). The results for Region B are 4.8×10^{16} cm^{-2} and 1.4×10^{16} cm^{-2} for $f = \frac{1}{2}$, $\alpha = 2$ and $f = \frac{1}{2}$, $\alpha = 1$, respectively. The space densities of $n(H_2)$ are obtained by dividing $N(^{13}CO)$ by ϵ times the source size, and are equal to 5.6×10^4 cm^{-3} and 1.7×10^4 cm^{-3} for the two cases. The masses are then ~ 4 or $\sim 2\, M_\odot$. Of course, all of these numbers depend sensitively on the value of f.

In analogy with the arguments presented above for Region A, the high-density case ($f = \frac{1}{2}$, $\alpha = 2$) in Region B requires that internal thermal pressure balance the external pressure, while the low-density case ($f = \frac{1}{2}$, $\alpha = 1$) requires that pressure balance be maintained with internal magnetic fields or turbulence.

Thus Region B could be in pressure equilibrium with the bright rim, if it is (*a*) spherical and supported by thermal pressure (due to the high resultant densities) or (*b*) filamentary and supported at a lower density by internal turbulence (or magnetic fields with an Alfvén velocity $v_A > \Delta v$). The derived excitation temperature (from eq. [5]) for the case of an unresolved sphere is

unusually large, however, and the filamentary model may be preferred. Since its velocity differs by about 1 km s^{-1} from other CO emission to the west of the bifurcation, Region B may be a small neutral fragment or filament that has broken off from the main cloud.

IV. BOUNDARY INSTABILITIES AT THE IONIZATION FRONT

The southern boundary of the molecular cloud shown in Figure 1*b* is very irregular. There are numerous regions where neutral gas seems to protrude into the H II region. This is reminiscent of a Rayleigh-Taylor instability, but the bright-rim instability of Kahn (1958) is probably more appropriate. This instability occurs when the ionizing flux increases with time. Our reanalysis of this problem suggests that the instability may be quite important here. The additional influence of a Kelvin-Helmholtz instability, as suggested by Osterbrock (1957), is also considered. The possibility that magnetic fields play a role in the deformation of ionization fronts, as considered by Okamoto (1968), is then briefly discussed.

Kahn (1958) showed that an ionization (*I*) front (without magnetic fields) may be unstable, if the incident Lyman continuum flux increases with time. However, he pointed out that absorption in the bright rim will tend to stabilize it, unless the Lyman continuum flux from a normal OB star or association increases at an unrealistically large rate. Since he considered only the relatively slow flux changes due to stellar evolution, he concluded that the instability could not be responsible for the bright-rim phenomena associated with OB clusters.

The required rapid increase of ionizing flux may be present in our case. We proceed in a slightly different manner than Kahn, using an isothermal equation of state in the neutral gas and writing the time-dependent pressure at the *I* front directly in terms of the separation between the star and the cloud. The assumption of isothermal changes is applicable, because the cooling rates in the dense gas ahead of the ionization front are large compared with the dynamical rates of interest. The use of pressure at the *I* front automatically includes any stabilizing tendencies due to absorption in the H II region.

Consider a planar, *D*-critical ionization front (see Kahn 1954 for nomenclature) advancing into a neutral region. A shock that may precede the front is not important for the present calculation, so we assume here that such a shock is sufficiently far in advance of the *I* front to be ignorable. The speed of advance of a *D*-critical ionization front into the neutral gas is (Spitzer 1968)

$$u = c^2/2c_{\rm II} \tag{6}$$

for sound speeds c and $c_{\rm II}$ in the neutral and ionized regions, respectively.

The pressure at the ionization front, P_i, depends almost exclusively on the electron density there, which continuously adjusts to changes in the incident flux. For the ionization of clouds by nearby O stars, we have to a good approximation

$$n_e(t)^2\alpha\Delta \approx \frac{S}{4\pi R(t)^2} \tag{7}$$

for effective thickness of the H II region Δ, for hydrogen recombination coefficient α, and for Lyman continuum luminosity S in photons s^{-1}, of a source at a distance R from the cloud. The effective thickness Δ depends on the geometry and size of the cloud, and it will not change much in the 5×10^5 to 1×10^6 year time interval we are considering. The pressure exerted on the neutral cloud then scales with $R(t)^{-1}$ as the star moves. We use simply

$$P_i(t) = \frac{P_0R_0}{R(t)} \tag{8}$$

for some normalization constants P_0 and R_0.

For time-dependent external pressures, the pressure in the neutral gas ahead of the ionization front P_n is a function of distance x measured from the front into the neutral cloud. Since the pressure wave ahead of the ionization front moves with speed c, we have for the pressure in the unperturbed neutral gas

$$P_n(t, x) = P_i(t - x/c) = \frac{P_0R_0}{R(t - x/c)} \cdot \tag{9}$$

Here $R(t - x/c)$ represents the distance between the cloud and the star at the time $t - x/c$.

Now consider a sinusoidal perturbation of the *I* front such that the front is displaced from a plane by the distance δ at the coordinate y measured along the surface. Positive δ corresponds to a displacement of the surface in the x direction. We assume that this corrugation extends for an effective depth $1/\eta$ below the surface and has the form (Kahn 1958)

$$\delta(t, x, y) = \delta_0 \exp\left[\gamma t - \eta(x - ut)\right] \cos(ky) . \tag{10}$$

The pressure at the point (x, y) below the average plane of the surface at the time t is then given by $P_n[t, x - \delta(t, x, y)]$, which may be expanded to first order in the perturbation:

$$P_n[t, x - \delta(t, x, y)] = P_n(t, x) + P_1(t, x, y) , \tag{11}$$

where

$$P_1(t, x, y) = \frac{\delta(t, x, y)}{c} \left(\partial P_i/\partial t\right)|_{(t - x/c)}$$

$$= \frac{\delta(t, x, y)v_0P_0R_0}{cR(t - x/c)^2} \ll P_0(t, x) ; \tag{12}$$

$v_0 = -dR/dt$ is the stellar velocity.

Gradients in the perturbed pressure P_1 cause an acceleration of the perturbation:

$$\frac{\partial^2\delta}{\partial t^2} = -\frac{c^2}{P_n}\frac{\partial}{\partial x}P_1 . \tag{13}$$

With equations (11) and (12), this becomes

$$(\gamma + \eta u)^2 = \frac{cv_0}{R(t - x/c)}\left[\eta + \frac{2v_0}{cR(t - x/c)}\right]. \quad (14)$$

The equation of continuity may be combined with the above force equation to give the wave equation

$$\frac{1}{c^2}\frac{\partial^2}{\partial t^2}P_1 = \frac{\partial^2}{\partial x^2}P_1 + \frac{\partial^2}{\partial y^2}P_1, \quad (15)$$

which may be reduced to

$$\frac{1}{c^2}\left[\gamma + \eta u + \frac{2v_0}{R(t - x/c)}\right]^2 = \left[\eta + \frac{2v_0}{cR(t - x/c)}\right]^2 - k^2. \quad (16)$$

Now suppose $\gamma = gv_0/R$ and $\eta = nv_0/cR$. In the appropriate limit of $u \ll c$, equations (14) and (16) give

$$g^4 - (g + 2)^2 = (ckR/v_0)^2, \quad (17)$$

$$n = g^2 - 2, \quad (18)$$

which may be solved for g and n.

For typical values of c, k, R, and v_0, the right-hand side of equation (17) is much less than 1. Then

$$g \approx 2 + \frac{1}{24}\left(\frac{ckR}{v_0}\right)^2. \quad (19)$$

In particular, for $c = 0.26$ km s^{-1} at $T = 19$ K, $R \approx 5$ pc, $k \approx (2\pi/1$ pc), and a stellar velocity with respect to the cloud of $v_0 \approx 50$ km s^{-1}, we obtain $(g - 2) \approx 10^{-3}$. Thus the growth rate is nearly independent of perturbation length for parsec-size perturbations and typically equals

$$\gamma \approx 2v_0/R \quad (20)$$

for R equal to the instantaneous separation between cloud and star.

For ξ Per, with an estimated $v_0 \approx 50$ pc, the growth time $\gamma^{-1} = 4.9 \times 10^4$ years at present and $\gamma^{-1} = 2 \times 10^5$ years when ξ Per first became a runaway, some 20 pc/$v_0 \approx 4 \times 10^5$ years ago. Evidently long-wavelength perturbations have a growth time that is always a factor of 2 less than the time before the (effective) instant of nearest approach, R/v_0. This is interesting, for it suggests that, if no additional source of steady ionization dilutes the increase in the flux from a moving star, then ionization fronts formed by these stars may be unstable, regardless of the stellar velocity.

Once this surface instability begins, elements of neutral gas which protrude into the H II region may become very narrow as a result of a Kelvin-Helmholtz instability and eventually may pinch off from the rest of the cloud. Osterbrock (1957) discussed this possibility in the context of a maximum length for the elongation of "elephant trunks," often visible in active H II regions.

We estimate that the time scale for this process to occur will be the growth time of a Kelvin-Helmholtz instability at a surface which separates the cloud in Region B from the adjacent H II region. The particle densities on the two sides of this surface are taken to be $n_0 \approx 3000$ cm^{-3} and $n_e \approx 45$ cm^{-3}, respectively; the scale λ of the region is assumed to be roughly one beamwidth, or about 0.3 pc. The relative fluid flow along the surface is taken to be $\Delta v \approx 3$ km s^{-1}, which is consistent with the difference between the radial velocity of the H II region (Lynds 1969) and the average velocity of the cloud in Figure 1*b*. The time scale is then (Lamb 1945)

$$t_{KH} \approx \frac{\lambda}{2\pi\Delta v}\left(1.7\frac{n_0}{n_e}\right)^{1/2} \approx 1.5 \times 10^5 \text{ years}. \quad (21)$$

Since this is less than the expected travel time of ξ Per, Kelvin-Helmholtz instabilities may have influenced the development of Region B, as well as other irregularities at the ionization front. As shown in § III, Region B may have already been pinched off from the cloud and may now be a small, unresolved neutral filament.

The stability of an ionization front in the presence of a magnetic field has been studied by Okamoto (1968). He determined that instabilities leading to fragmentation can exist, if the field is in the plane of the ionization front. Perturbations perpendicular to the direction of the field would grow, while those parallel to the field would damp out. The average interstellar field orientation on the line of sight to ξ Per has been determined from polarization studies to be roughly aligned on a N-S axis (Hall 1954). If this direction were the same 1° to the north of ξ Per, in the dark cloud L1449, then B would be perpendicular to the plane of the ionization front (i.e., parallel to the bifurcation) and Okamoto's results would not be applicable. However, if a strong isothermal shock precedes the *I* front into the neutral cloud, then the postshock field may be oriented along the *I* front regardless of the direction of the preshock field. Okamoto's instability could then lead to the bifurcation seen in Figure 1. Unfortunately, the field orientation closer to the ionization front or in the adjacent dark cloud is not yet known.

If the field is perpendicular to the ionization front, then Kahn's instability could be mildly suppressed. However, such a field would enter only into the transverse force in the wave equation (eq. [15]), which is proportional to k^2; so large perturbations would still grow at the rate given by equation (20). The action of a magnetic field would be to increase the size of the most rapidly growing perturbations by roughly v_A/c. The maximum growth rate in Kahn's analysis occurs for very small wavelengths, of the order $cR/v_0 \approx 0.02$ pc. Instabilities of this size may be present, but they would not result in the large-scale irregularities seen in Figure 1*b*. The inclusion of a magnetic field would bring into better agreement the unstable sizes determined by pressure gradients in the cloud and those observed in Figure 1*b*.

V. CONCLUSIONS

A ^{12}CO map with 2.'7 resolution has been made of a dark cloud adjacent to the California Nebula (NGC 1499), which is ionized by the runaway star ξ Per. The results showed the presence of some internal velocity structure, possibly related to the action of the ionization front. The region was also sampled in ^{13}CO, CS, and H_2O maser emission (no H_2O was detected). Column densities of ^{13}CO were determined from the data, and the standard method of conversion to H_2 column densities was discussed. Estimates of star counts confirmed the value of $N(^{13}CO)/N(H_2) \approx 2 \times 10^{-6}$, characteristic of regions with relatively low extinction.

Arguments relating to pressure balance across the ionization front implied that a small, protruding region at the southern edge of the cloud (Region B) is unresolved. Scaling arguments were then used to show that, if the gas in Region B is spherically symmetric, then its internal pressure is probably thermal in origin; if the region is filamentary (linear), then the internal pressure is probably due to turbulence or magnetic fields.

The boundary of the cloud at the ionization front is highly irregular, and several instabilities which could have caused the observed structure were discussed. In particular, the time-dependent flux of a rapidly moving star like ξ Per was shown to provide unstable conditions at such an ionization front. The time scale for growth of this instability is less than the travel time of the star. We also noted that Region B could have been shaped and, possibly, pinched off from the main cloud by a Kelvin-Helmholtz instability.

The authors gratefully acknowledge support from an Amelia Earhart Graduate Fellowship of Zonta International (D. M. E.) and the Society of Fellows at Harvard University (B. G. E.).

REFERENCES

Arons, J., and Max, C. E. 1975, *Ap. J. (Letters)*, **196**, L77.
Bohnenstengel, H.-D., and Wendker, H. J. 1976, *Astr. Ap.*, **52**, 23.
Chaisson, E. J. 1975, *Ap. J. (Letters)*, **197**, L65.
Davis, J. H., and Vanden Bout, P. 1973, *Ap. Letters*, **15**, 43.
Dickman, R. L. 1975, Ph.D. thesis, Columbia University.
Elmegreen, B. G., and Lada, C. J. 1976, *A.J.*, **81**, 1089.
Encrenaz, P. J., Falgarone, E., and Lucas, R. 1975, *Astr. Ap.*, **44**, 73.
Gottlieb, C. A., Lada, C. J., Gottlieb, E. W., Lilley, A. E., and Litvak, M. M. 1975, *Ap. J.*, **202**, 655.
Hall, J. S. 1954, Liège Colloquium No. 5, "Procèsses nucléaires dans les astres," *Mém. Soc. Roy. Sci. Liège*, Sér. 4, **13**, 543.
Jenkins, E. B., and Savage, B. D. 1974, *Ap. J.*, **187**, 243.
Kahn, F. D. 1954, *Bull. Astr. Inst. Netherlands*, **12**, 187.
———. 1958, in IAU Symposium No. 8, "Cosmical Gas Dynamics," in *Rev. Mod. Phys.*, **30**, 1058.
Knapp, G. R., and Jura, M. 1976, *Ap. J.*, **209**, 782.
Knapp, G. R., Kuiper, T. B. H., Knapp, S. L., and Brown, R. L. 1977, *Ap. J.*, **214**, 78.
Lada, C. J. 1976, *Ap. J. Suppl.*, **32**, 603.
Lamb, H. 1945, *Hydrodynamics* (New York: Dover).
Langer, W. D. 1977, *Ap. J. (Letters)*, **212**, L39.
Liszt, H. S., and Linke, R. A. 1975, *Ap. J.*, **196**, 709.
Lynds, B. T. 1962, *Ap. J. Suppl.*, **7**, 1.
———. 1969, *Pub. A.S.P.*, **81**, 496.
Okamoto, I. 1968, *Pub. Astr. Soc. Japan*, **20**, 122.
Oppenheimer, M., and Dalgarno, A. 1975, *Ap. J.*, **200**, 419.
Osterbrock, D. E. 1957, *Ap. J.*, **125**, 622.
Penzias, A. A., Solomon, P. M., Wilson, R. W., and Jefferts, K. 1971, *Ap. J. (Letters)*, **168**, L53.
Pottasch, S. 1956, *Bull. Astr. Inst. Netherlands*, **13**, 77.
Scoville, N. Z., Solomon, P. M., and Penzias, A. A. 1975, *Ap. J.*, **201**, 352.
Shinohara, M., and Ishida, K. 1976, *Pub. Astr. Soc. Japan*, **28**, 437.
Spitzer, L., Jr. 1968, *Diffuse Matter in Space* (New York: Interscience).
Tucker, K. D., Dickman, R. L., Encrenaz, P. J., and Kutner, M. L. 1976, *Ap. J.*, **210**, 679.
van Rhijn, P. J. 1929, *Groningen Pub.*, **43**, 1.
Wannier, P. G., Penzias, A. A., Linke, R. A., and Wilson, R. W. 1976, *Ap. J.*, **204**, 26.

BRUCE G. ELMEGREEN and DEBRA MELOY ELMEGREEN: Center for Astrophysics, Harvard College Observatory and Smithsonian Astrophysical Observatory, 60 Garden Street, Cambridge, MA 02138